Hydraulic modeling of runoff over a rough surface under partial inundation

Nicolas Roche, Jean-Francois Daian, D. S. L. Lawrence

Hydraulic modeling of runoff over a rough surface under partial inundation

N. Roche,[1] J.-F. Daïan,[1] and D. S. L. Lawrence[2]

Received 31 August 2006; revised 27 February 2007; accepted 25 April 2007; published 11 August 2007.

[1] This study presents a numerical method to derive the Darcy-Weisbach friction coefficient for overland flow under partial inundation of surface roughness. To better account for the variable influence of roughness with varying levels of emergence, we model the flow over a network which evolves as the free surface rises. This network is constructed using a height numerical map, based on surface roughness data, and a discrete geometry skeletonization algorithm. By applying a hydraulic model to the flows through this network, local heads, velocities, and Froude and Reynolds numbers over the surface can be estimated. These quantities enable us to analyze the flow and ultimately to derive a bulk friction factor for flow over the entire surface which takes into account local variations in flow quantities. Results demonstrate that although the flow is laminar, head losses are chiefly inertial because of local flow disturbances. The results also emphasize that for conditions of partial inundation, flow resistance varies nonmonotonically but does generally increase with progressive roughness inundation.

Citation: Roche, N., J.-F. Daïan, and D. S. L. Lawrence (2007), Hydraulic modeling of runoff over a rough surface under partial inundation, *Water Resour. Res.*, *43*, W08410, doi:10.1029/2006WR005484.

1. Introduction

[2] Shallow water flows over surfaces with emergent roughnesses are of great significance in the transfer of soluble and particulate contaminants from land surfaces to channelized watercourses. In standard models of overland flow at the watershed scale, resistance to the flow is characterized by a friction coefficient, e.g., the Darcy-Weisbach friction factor, and is based on an analogy with resistance to flows in pipes. This analogy is correct when the roughness has a characteristic length which is significantly less than the flow depth, as previous laboratory experiments and theoretical analyses have shown [*Horton et al.*, 1934; *Woo and Brater*, 1961; *Emmett*, 1970; *Yoon and Wenzel*, 1971; *Li and Shen*, 1973; *Phelps*, 1975; *Savat*, 1980]. However, when the flow depth and the boundary roughness are of the same order of magnitude, the analogy with one-dimensional flows in pipes is weak because of the variable influence of the roughness surface as the degree of roughnesses submergence varies.

[3] It has been established for some time that boundary resistance is pivotal in determining the discharge-depth relationship in overland flow. *Emmett* [1970] demonstrated that the hydraulic geometry approach developed for fluvial hydraulics by *Leopold and Maddock* [1953] is also suitable for overland flow hydraulics. Subsequently, *Richards* [1973] proposed a log-quadratic form of the discharge versus depth relationship (where d is the depth, Q the discharge and f_1, f_2, f_3 are numerical constants):

$$\log(d) = f_1 + f_2\log(Q) + f_3(\log(Q))^2 \quad (1)$$

Nevertheless, the frictional resistance continued to be assessed via a Darcy-Weisbach coefficient principally as a function of the Reynolds number.

[4] In 1991, *Gilley and Finkner* [1991] proposed that, to better account for the dominant influence of roughness on flow resistance, empirical expressions for Darcy-Weisbach and Manning coefficients based on a roughness characteristic length scale (i.e., the random roughness) could be used. However, the two formulas they suggested are empirical, rather than derived from physical principles, and so, do not significantly advance our understanding of overland flow resistance. Additionally, *Takken and Govers* [2000] subsequently demonstrated that the random roughness is not a satisfactory length scale for characterizing the surface roughness for use in these formulas.

[5] An evaluation of the friction coefficient solely as a function of Reynolds number can produce apparent trends between resistance and flow Reynolds number. These trends have even been interpreted as indicative of laminar versus turbulent flow regimes, on the basis of analogies with pipe flow hydraulics [*Dunne and Dietrich*, 1980]. However, as suggested by *Abrahams et al.* [1986] and systematically evaluated by *Lawrence* [1997], these trends are artifacts of the experimental design. They are erroneously attributed to the influence of Reynolds number while they are in fact due to the varying flow depth and associated degree of roughness submergence during successive experimental runs.

[6] *Lawrence* [1997] suggested a systematic theory with physical bases for characterizing shallow flows on very rough surfaces. Considering similarity theory and simple

[1] Laboratoire d'Étude des Transferts en Hydrologie et Environnement, Université Joseph Fourier, France.
[2] School of Human and Environmental Sciences, University of Reading, Reading, UK.

0043-1397/07/2006WR005484

scaling arguments, Lawrence proposed that the inundation ratio (Λ) should be regarded as the criterion for selection of the various flow regimes, rather than the Reynolds number. The inundation ratio is the relationship between the flow depth (d) and the roughness characteristic size (k):

$$\Lambda = \frac{d}{k} \tag{2}$$

[7] As an alternative to the classification according to the Reynolds number, Lawrence distinguishes three flow regimes according to the inundation ratio [*Lawrence*, 1997].

[8] 1. For well inundated flow, rough turbulent flows formula proposed by Nikuradse is used.

[9] 2. At marginal inundation, the friction coefficient decreases very quickly while the flow depth increases.

[10] 3. Finally, at partial inundation, the friction coefficient is proportional to the cover rate of surface by roughnesses, to the inundation ratio and to the drag coefficient of a half sphere.

[11] In subsequent work, *Lawrence* [2000] proposed a general form of the functional relationship between the resistance and the inundation ratio for surfaces with two discrete, well-defined roughness length scales. The resulting "modified mixing length model" has been successfully applied to estimate flow resistance during marginal inundation of well-characterized surfaces. This work has been further applied and extended by *Ferro* [2003] to explicitly incorporate free surface effects based on the Froude number for the flow.

[12] In 2000, *Takken and Govers* [2000] conducted a series of experiments on rough surfaces, but did not find the ascending part of the curve proposed by Lawrence for partial inundation. They proposed an alternative numerical model in which they apply the Savat algorithms [*Savat*, 1980] only to the submerged parts of the surface. In addition, they proposed that the "equivalent roughness" could be optimized in order to improve the prediction of flow velocity.

[13] As the case of partial inundation still remains poorly characterized, the present study aims to develop a physically based numerical model accounting for the varying influence of roughness as the average height of the free surface varies. For this purpose, the model proposed here assumes that the free surface flow takes place in channels interconnected in a two-dimensional network. Within each channel, the classical laws of free surface hydraulics are assumed to apply and to vary with the local Reynolds number and local Froude number of the flow. A discharge conservation condition applied at each node of the network allows the global discharge and the Darcy-Weisbach coefficient to be estimated.

2. Network Based on the Free Surface Level

[14] Our main purpose is to better account for the varying influence of surface roughness on resistance as the level of the free surface progressively submerges a larger fraction of the rough boundary and the flow network evolves as new pathways become available. To assist in developing a numerical model for this evolution, a 60 cm $\times$ 60 cm sample of a quasi-natural surface was obtained by taking a mould of a sample of an asphalt car park surface. Using a laser roughness meter (with a precision of 10^{-2} mm), a height numerical map (HNM) of the sample with a grid of 1 mm $\times$ 1 mm was constructed. A medium base level for the rough surface was defined by the mean of the least squares fit to the roughness data. Accordingly, an average flow free surface height can be represented by a plane parallel to this base level plane. For each free surface level, a submerged region map (SRM) is computed (Figure 1).

[15] On these maps the submerged region appears in black. For each map, i.e., for each free surface height, we can distinguish areas which are likely to be below this height, and thus are likely to be inundated. On the basis of these data, we can then identify likely channels. Using discrete geometry as applied in image analysis [e.g., *Chassery and Montanvert*, 1991; *Coster and Chermant*, 1989; *Gonzales and Wood*, 1992], one can extract a "skeleton" of a given region within an image. The skeleton is a topological object built without any hydraulic consideration, but can be used to provide the general structure of the flow network. This two-dimensional concept has been used particularly in the study of transfer in porous media [*Laurent and Frendo-Rosso*, 1992] and an extended three-dimensional version was proposed by *Pieritz* [1992]. In the present study, the skeleton of the SRM is used for defining possible pathways for the flow for a given average free surface height. For practical implementation of the method of skeletonization, we used the free software: ImageJ (v 1.32J, Wayne Rasband, National Institutes of Health, USA).

[16] The evolution of the SRM and of its skeleton with increasing water depth (Figure 2) clearly shows a percolation process. Considering the increasing inundation of the surface, from the level corresponding to the lowest until the highest roughness, we observe the gradual appearance of submerged areas. Initially, these areas are not connected and no continuous pathway from one side of the surface to another is available for the flow. As the free surface level rises, the submerged areas become interconnected at a given stage, analogous to a "percolation threshold," a continuous pathway is created. The free surface level where this first way appears can be called the "percolation plane."

[17] Note that we are not attempting to model the gradual accumulation of water on the rough surface exposed to rain prior to the onset of the flow when the percolation stage is reached. We are considering only a stationary flow across the surface sample of a given discharge supplied at the upstream boundary of the sample.

[18] The flow network based on the skeletons is defined by edges and nodes. It was also necessary to define boundary nodes at the entry and exit of the flow domain. We identify nodes and edges on skeletons using discrete geometry considerations [*Chassery and Montanvert*, 1991; *Coster and Chermant*, 1989; *Gonzales and Wood*, 1992].

[19] On the bulk skeletons obtained, there are a lot of redundant nodes and edges, such as those which are not linked to both of the entry and exit side of the sample and will therefore not contribute to the hydraulic model. There are also a lot of branchings, connected to both sides, but which will also not be available for the flow. These supernumerary nodes and edges must be removed (Figure 3).

[20] Once this pretreatment is completed, we have the basis for the network, i.e., the functional nodes and the

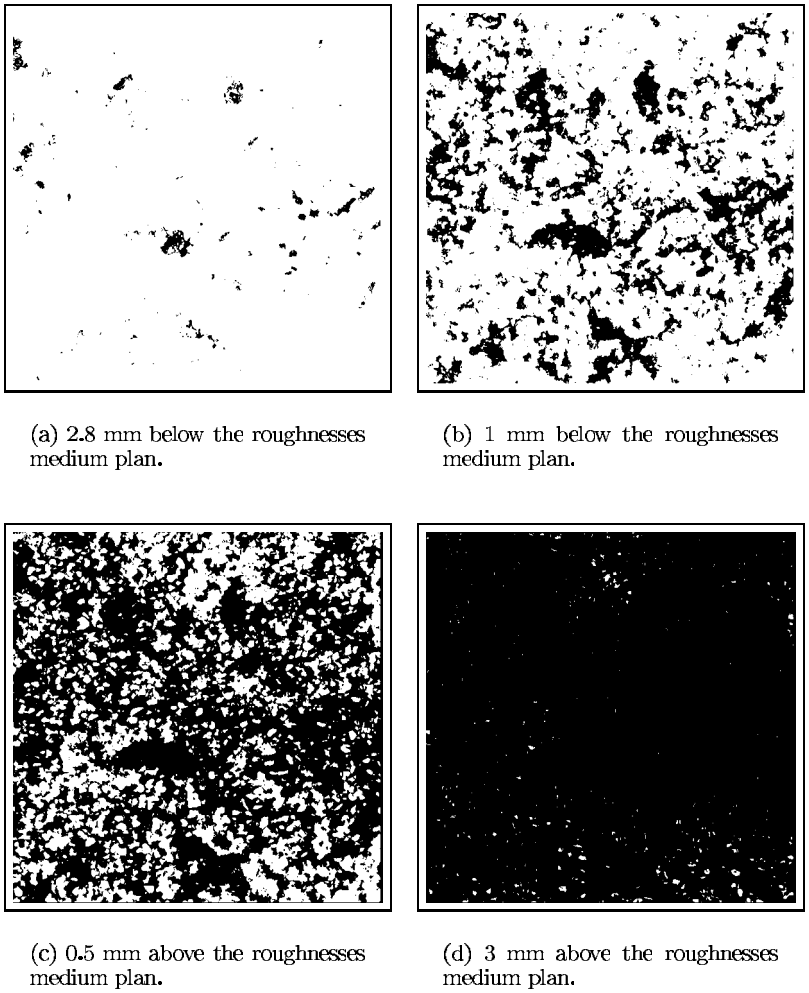

(a) 2.8 mm below the roughnesses medium plan.

(b) 1 mm below the roughnesses medium plan.

(c) 0.5 mm above the roughnesses medium plan.

(d) 3 mm above the roughnesses medium plan.

Figure 1. Submerged roughness maps for various free surface levels.

edges. It is then necessary to specify the parameters required for the hydraulic model for each edge in the network.

3. Hydraulic Model

[21] For each network corresponding to an average free surface level, we apply a hydraulic model in order to calculate the discharge on the surface sample for a steady state flow. The main assumption underlying the method adopted is that each node functions as a quasi-hydrostatic tank supplied and drained by edges which function as open channels. The hydraulic head at each node is used to drive the equations governing flow within each channel and the discharge in the channel must satisfy the discharge conservation law at each node. These flow laws and continuity constraints are applied using an iterative approach. Our model principle is very similar to hydrologic routing techniques considering cascade of reservoirs [*U.S. Army Corps of Engineers*, 1994].

3.1. Hydraulic Properties of the Network

[22] For a given average free surface level, we assume that flow will occur through the network corresponding to that level. However, in order to solve the flow problem, the hydraulic characteristics of each channel in the network must be specified. Particularly, it is necessary to locate the throat which may control the discharge in the case of critical flow and to define the throat cross-sectional area for each free surface level.

[23] The throats are determined using the distance map of the SRM. On the distance maps, each point is labeled according to its distance to the nearest point of the emerged region, also called the ''background'' of the image. Emerged region corresponds to the white part of the SRM (Figure 1). For a given edge, the throat, i.e., the narrowest cross section, should be located at the point of the edge which has the minimum distance to background. Although this point is obtained from a two-dimensional map of the free surface undisturbed by the flow, we assume that the corresponding cross section controls the flow in the channel.

[24] An equivalent triangular cross section located at the throat is defined using the HNM, by conserving the area and the width of the actual cross section. The vertex of this triangle is considered as the reference level for defining the water level y along the channel, and particularly the levels y_{us} in the upstream tank and y_{ds} in the downstream tank. For each step of the iterative method the equivalent cross section is calculated on the basis of the throat water depth y_{th}.

3.2. Flow Balance and Iterative Method

[25] The heads (or water levels) h_i (Table 1) at the nodes are unknown, and so, are determined by an iterative method. To initialize the water levels h_i we consider the undisturbed

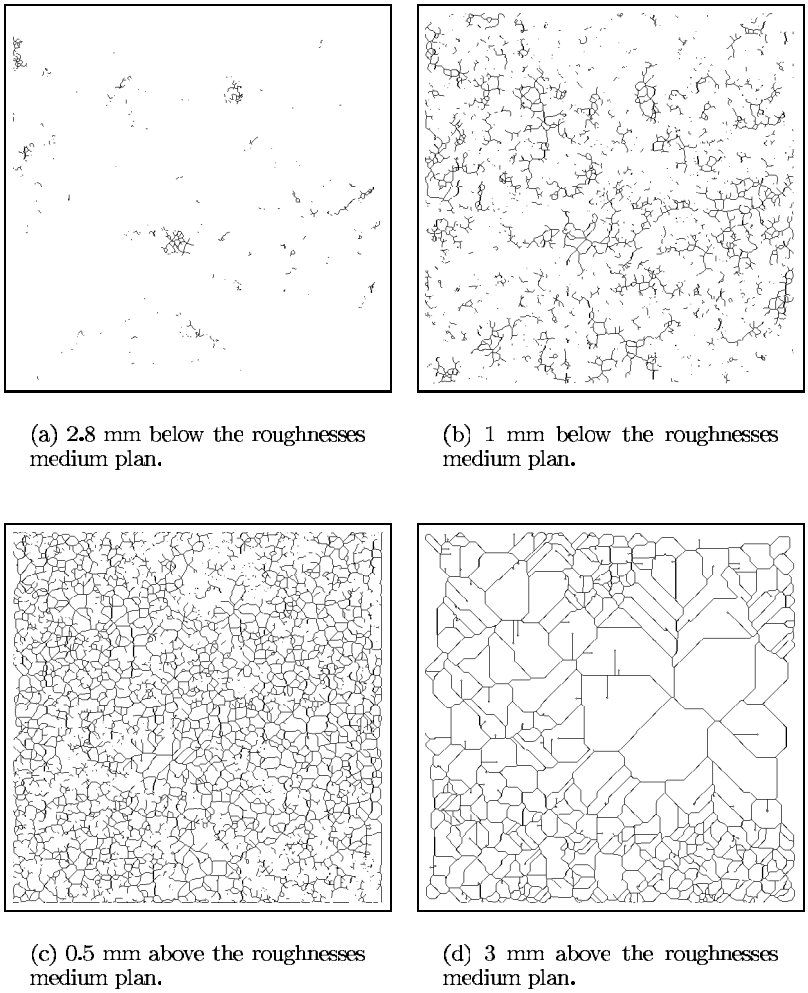

(a) 2.8 mm below the roughnesses medium plan.

(b) 1 mm below the roughnesses medium plan.

(c) 0.5 mm above the roughnesses medium plan.

(d) 3 mm above the roughnesses medium plan.

Figure 2. Skeletons of the submerged roughness maps.

free surface used for the generation of the SRM and its skeleton. The heads are allowed to slightly vary above or below the planar free surface in order to satisfy the governing laws. These variations have a negligible influence on the SRM and its skeleton. To solve the hydraulic problem, the head at the boundary nodes is maintained at zero at the downstream end of the sample and at a constant value H at the upstream end of the sample. H is depending on the slope of the roughnesses medium plane. H is the global head loss on the surface and our model calculate the corresponding discharge.

[26] At each iteration n, the previous head at each node is known (h_i^{n-1}). Then, according to the flow equations defined below (see paragraph 3.3), the discharge Q_{ij} through each edge ij located between the nodes i and j can be computed. Then, for each node we calculate the algebraic sum of the discharges supplying and draining it (Q_i):

$$\forall i \quad Q_i = \sum_{j \in E} Q_{ij} \tag{3}$$

where E is the set of the nodes connected to the node i by one or more edges.

[27] By convention, $Q_{ij} \geq 0$ when the flow occurs from node i to node j. So, if $Q_i \geq 0$, the outgoing flow of the node i is more important than the entering one. For steady state, all the Q_i must be zero. To obtain this result, at the iteration step n, the variation of the head at each node is calculated as follows:

$$h_i^n = h_i^{n-1} - \alpha Q_i \tag{4}$$

where α is an arbitrary capacity coefficient fitted in order to obtain a regular convergence of the algorithm.

[28] So at each step n of the iterative method we need to calculate the local discharge (Q_{ij}) on each edge according to the nodes head. On each edge the local discharge is known by calculating the throat water depth y_{th} and velocity v_{th} on the basis of the upstream and downstream nodes head:

$$Q_{ij} = v_{th} S(y_{th}) \tag{5}$$

3.3. Flow and Head Loss in a Channel

[29] The nature of the flow in a given edge ij of the network and the subsequent head loss are determined by the heads h_i and h_j at the upstream and downstream nodes (then they are respectively written h_{us} and h_{ds}), or the corresponding local water depths y_{us} and y_{ds}. Depending on these depths, the flow may be subcritical or critical at the throat [*Lencastre*, 1979], laminar or turbulent. These various flow regimes are identified by the local Froude and Reynolds numbers, both calculated at the throat of the channel. For the case of subcritical flow, the head loss is

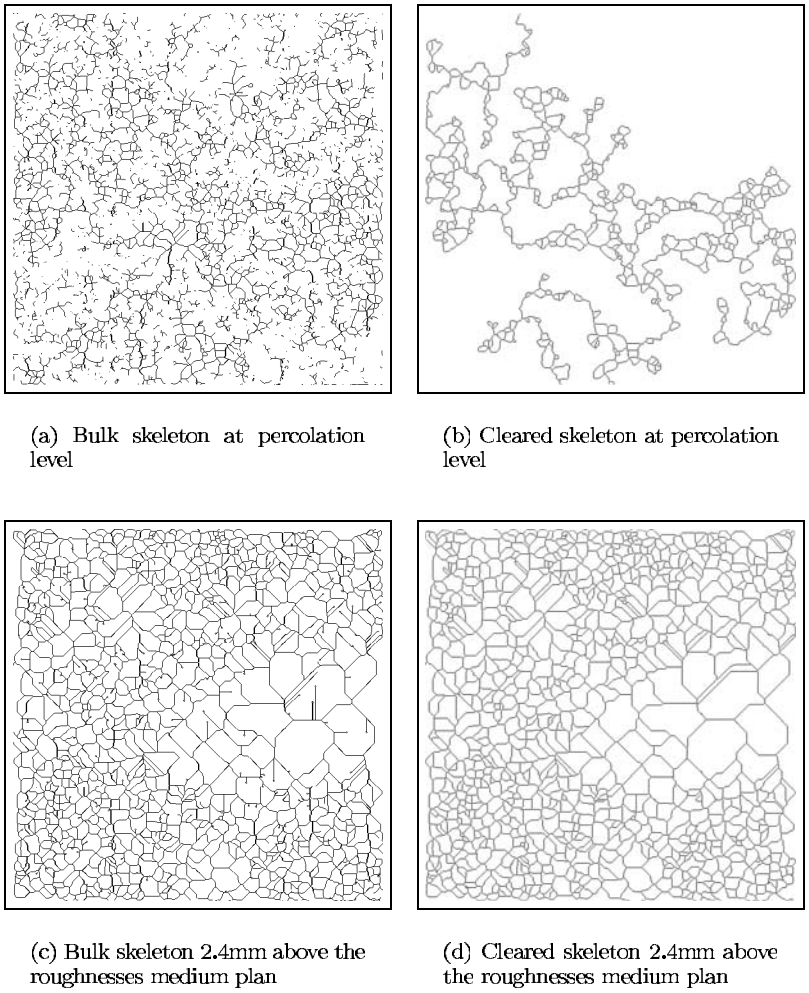

Figure 3. Clearing the skeletons. This step simplifies the network and has significant consequences near the percolation level.

due primarily to frictional resistance, and will vary depending on whether the flow is laminar or turbulent. Where the flow reaches criticality (i.e., when Fr = 1) a local hydraulic jump or a water fall will appear in the zone downstream of the throat, and inertial losses will locally dominate. However, although we consider two principal sources of head loss (friction and inertial), their respective contributions at the scale of the entire network cannot be distinguished in the value of the global friction coefficient. This is a difference between the approach we are using and that proposed by *Rauws* [1980] following the work of *Einstein and Banks* [1950].

3.3.1. Subcritical Flow

[30] For subcritical flow, the water depth at the throat y_{th} and the fluid velocity v_{th} must satisfy the following two equations:

$$y_{th} + \frac{v_{th}^2}{2g} = y_{us} \tag{6}$$

$$h_{us} - h_{ds} = f'_{ij} \frac{L_{ij}}{D(y_{th})} \frac{v_{th}^2}{2g} \tag{7}$$

where y_{us} and y_{ds} are evaluated relative to a local reference defined by the vertex of the triangular throat cross section. L_{ij} is the edge length, $D(y_{th})$ is the throat hydraulic diameter (calculated considering the triangular section assumption) and v_{th} is the fluid velocity at the throat. f'_{ij} is the edge Darcy-Weisbach coefficient, we use the traditional formulas of Poiseuille in the laminar case and Blasius in the turbulent one.

Table 1. Hydraulic Model Nomenclature

Parameter	Description
h_i	head at node i relatively to an absolute reference
y_i	head at node i relatively to the edge bed at the throat
Q_i	discharge balance for the node i
y_{us}, y_{ds}	considering an edge of the network, subscripts *us* and *ds* refer to upstream node and downstream node, respectively
f'_{ij}	Darcy-Weisbach coefficient of the considered edge
L_{ij}	length of the edge between nodes i and j
Q_{ij}	discharge on the edge between nodes i and j
v_{th}	fluid velocity calculated at the throat of the considered edge v_{th} can be equal to v_{lam}, v_{turb} or v_{cr} when the flow regime is laminar, turbulent, or critical, respectively
y_{th}	water depth calculated at the throat of the considered edge y_{th} can be equal to y_{lam}, y_{turb} or y_{cr} when the flow regime is laminar, turbulent, or critical, respectively
$D(y_{th})$	throat hydraulic diameter calculated on the basis of y_{th}
$S(y_{th})$	throat cross section calculated on the basis of y_{th}

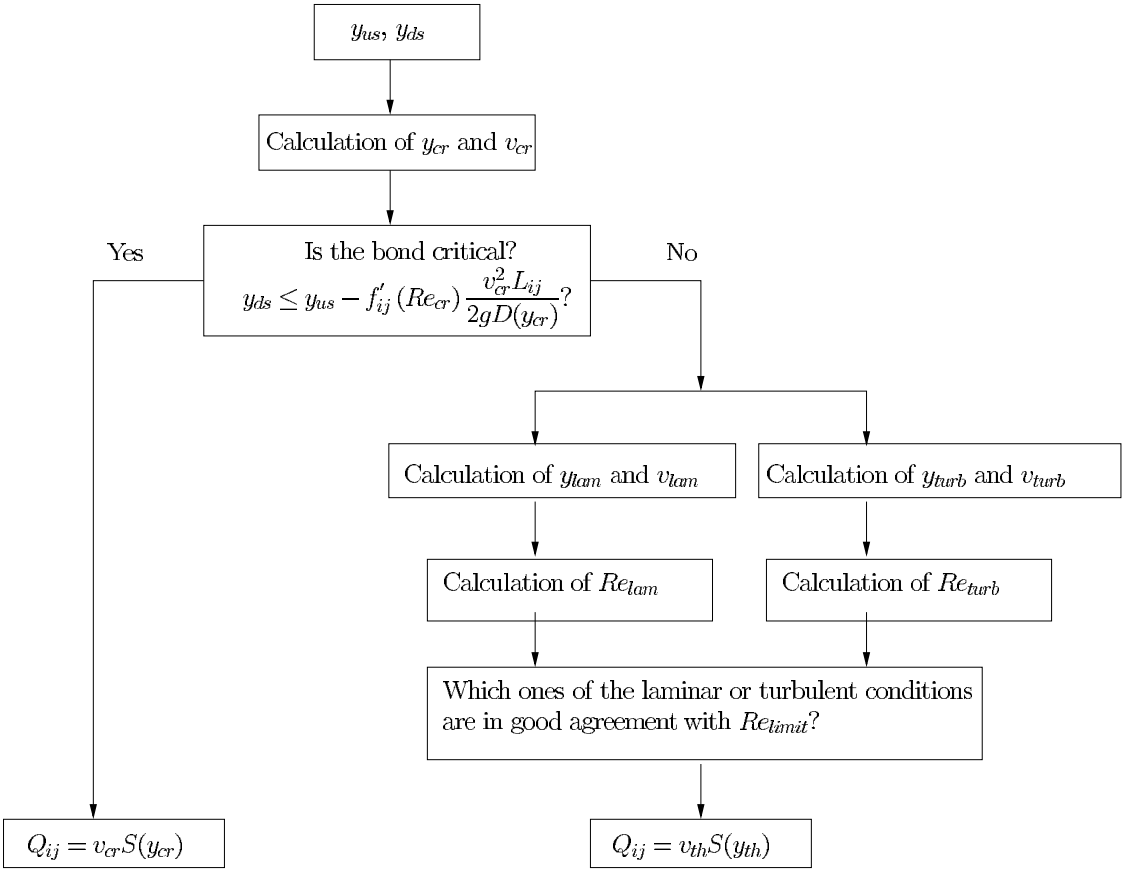

Figure 4. Calculation of the discharge on each edge of the network. Considering the y_{us} and y_{ds} of the iteration step, we determine whether the flow is critical or not. If the flow is subcritical, we calculate y_{th} and v_{th} for both laminar and turbulent conditions. Eventually, we choose which conditions are in good agreement with the laminar/turbulent transition by comparing the corresponding Reynolds numbers to Re_{limit}.

[31] Equation (7) deals with total head loss on the edge between upstream and downstream tank. For simplicity, we assume that the flow energy is conserved along the convergent part of the channel upstream of the throat and that frictional as well as inertial losses all occur downstream of the throat (equation (6)). Considering the resulting y_{th} and v_{th} we can then calculate the edge Reynolds number:

$$Re_{th} = \frac{v_{th} D(y_{th})}{\nu} \tag{8}$$

where v is the kinematic viscosity of water. Re_{th} is written Re_{lam}, Re_{turb} or Re_{cr} when the flow regime is respectively laminar, turbulent or critical.

[32] By applying the Poiseuille formula in the laminar case, where $f'_{ij} = \frac{64}{Re_{th}}$, we derive a polynomial equation (fourth degree) for the water depth at the throat which we solve using the Ferrari method [*Kurosh*, 1972]. For the turbulent case, where the Blasius formula gives frictional resistance as $f'_{ij} = \frac{0.316}{Re_{th}^{1/4}}$, we derive an algebraic equation which can be solved by trial and error on the interval [y_{cr}, y_{us}], as the function will behave monotonically in this region.

[33] The selection of laminar and turbulent mode is done a posteriori, since the fluid velocity and water height above the throat are needed to calculate Reynolds number. In the Moody diagram [*Moody*, 1944], there is a zone known as transition zone between the laminar and turbulent regimes, which has been ignored here for simplicity. Therefore, in order to avoid an abrupt jump in the friction coefficient value which might introduce a disturbance in the convergence of the iterative process, the Poiseuille and Blasius laws were extrapolated to their point of intersection. The resulting limit between the laminar and turbulent flow regimes is $Re_{limit} \simeq 1190$.

3.3.2. Critical Flow

[34] For a given upstream level y_{us}, with a lower value of the downstream level y_{ds}, the subcritical solution is valid until the critical conditions are reached at the throat. For a triangular section, this will occur when

$$y_{th} = y_{cr} = \frac{4}{5} y_{us} \quad and \quad v_{th} = v_{cr} = \sqrt{2g \frac{y_{us}}{5}} \tag{9}$$

The limiting value of y_{ds} is therefore

$$y_{ds} = y_{us} - f'_{ij} \frac{v_{cr}^2 L_{ij}}{2gD(y_{cr})} \tag{10}$$

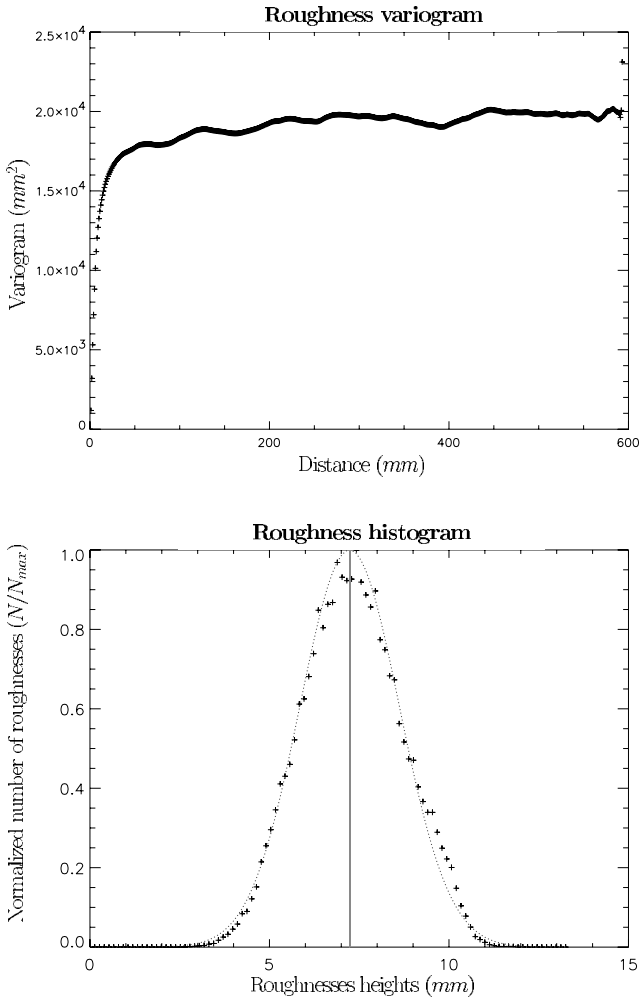

Figure 5. Statistical characteristics of our surface sample.

[35] If the downstream level becomes lower than this limiting value, the flow regime remains critical at the throat and supercritical flow occurs downstream of the throat. A hydraulic jump or waterfall occurs before the downstream tank and provides the additional head loss required to reach the downstream level y_{ds}. Consequently, the discharge in the channel is determined by the critical conditions corresponding to the upstream level and no further head loss computation is necessary.

[36] Figure 4 summarizes the strategy used for the computation of flow in each edge of the network.

4. Results

4.1. Roughness Characteristic Height

[37] In order to evaluate the discharge or Darcy-Weisbach coefficient as a function of a roughness inundation ratio, we need to define a single characteristic height for the surface roughnesses. The diameters d_{50} or d_{90} (the respective diameter of the ground particles for which 50 or 90 per cent are finer) have been used in the literature to define the inundation ratio [*Rauws*, 1980; *Abrahams et al.*, 1986; *Lawrence*, 1997].

[38] For the surface studied, we need to examine its statistical properties. To do this we calculate the variogram and histogram of roughnesses for the sample surface (Figure 5). These respectively characterize the degree of spatial autocorrelation in roughness heights and the frequency distribution of heights on the surface. The variogram reaches a plateau at about 50 mm, indicating that the largest roughness height length scale is significantly smaller than the sample size [*Kamphorst*, 2000], and the histogram is clearly unimodal such that the surface roughness is dominated by a single height length scale.

[39] The Gaussian form of the histogram also allows us to assume that 95% of the roughness heights are between $\mu - 2\sigma$ and $\mu + 2\sigma$ (where μ is the average size of roughnesses and σ their standard deviation). The reference chosen for the free surface level is the percolation plane, rather than the medium plane. To do so ensures that when $d = 0$, there is no discharge over the surface. Since the plane of percolation in our model of the HNM is close to the medium plane of the surface roughness, we can further choose to regard the standard deviation of the roughness heights standard deviation σ as the roughness characteristic height:

$$\Lambda = \frac{d}{2\sigma} \quad \text{with } \sigma = 1.38 \text{ mm} \tag{11}$$

where d is the varying water depth. When $\Lambda = 1$, we know that at least 95% of the surface roughness is inundated.

4.2. Heads

[40] One of the principal assumptions underlying our model relates to the free surface geometry, in that we assume that the free surface can be represented as a planar level. Therefore the variability in the local height of the free surface estimated by the iterative hydraulic model (Figure 6) must be sufficiently small, so as to not alter the derived flow network. Figure 6 represents the dimensionless altitude of the free surface at each node as a function of the distance to the downstream edge of the sample (for a 3% slope).

[41] The central line on each graph plane corresponds to the planar free surface level used to estimate the inundation ratio while the two other straight lines represent typical roughness height interval $\pm 2\sigma$. At lower inundation levels, the free surface is more variable and tends to be slightly lower than the head associated with a plane surface. This variability decreases with inundation, presumably because of the greater connectivity in the network, such that local isolated pools with a large drop in head across them are less frequent. In all cases the deviation in free surface elevation remains fairly small relative to the roughness height. Consequently, the approximation of the SRM on the basis of the undisturbed planar free surface appears to be valid.

4.3. Statistical Characterization of the Local Flow Parameters

[42] For each free surface level we calculate the velocity, Froude and Reynolds numbers at the throats. Local Reynolds numbers are calculated using equation (8) and local Froude numbers are calculated for the triangular throat section as

$$Fr_{th} = \frac{2v_{th}}{\sqrt{g y_{th}}} \tag{12}$$

For each variable Γ (i.e., v_{th}, Fr_{th}, Re_{th}), we compute a cumulative distribution function according to the discharge,

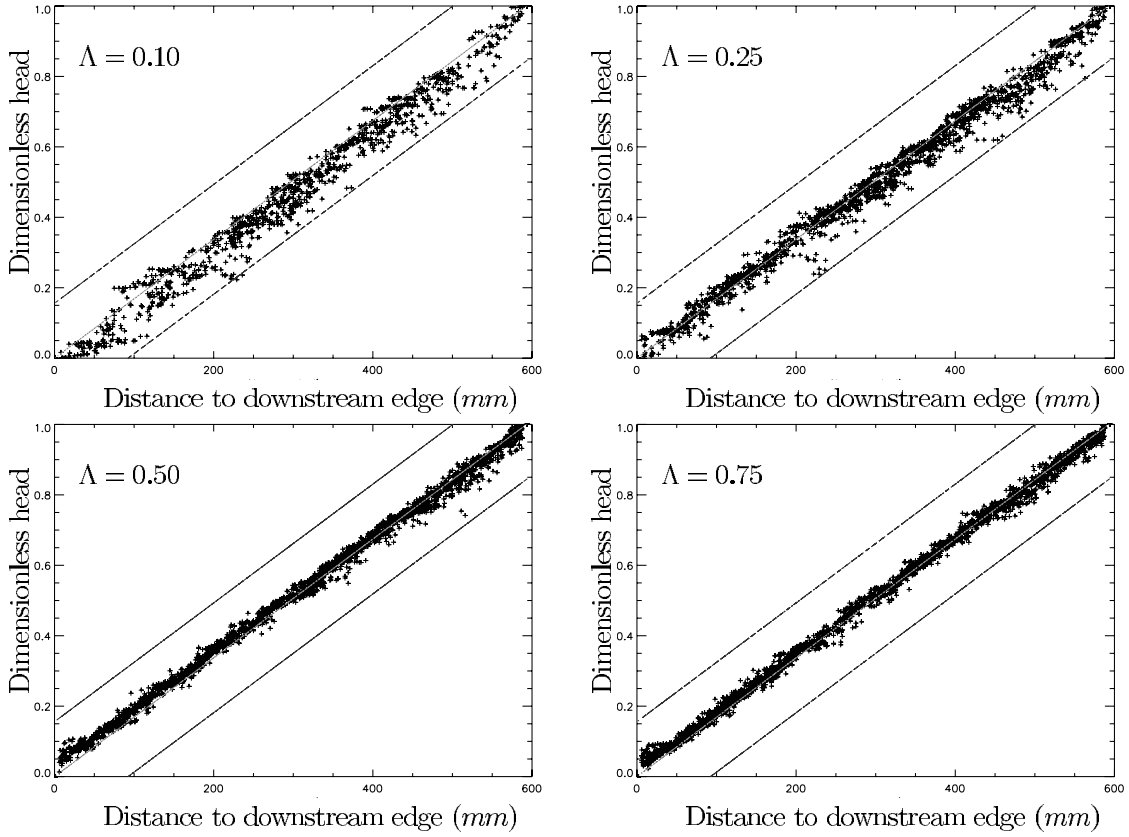

Figure 6. Dimensionless node head (h_i/H) estimated by the model for a 3% slope.

in order to enhance the influence of the significant edges participating in the flow:

$$F(X) = \frac{\sum_{\Gamma=0}^{\Gamma=X} Q_{ij}}{\sum_{\Gamma=0}^{\Gamma=\Gamma_{max}} Q_{ij}} \tag{13}$$

where

Q_{ij} discharge on the edge between nodes i and j;
Γ the local velocity or local Froude number (Figure 7) or local Reynolds and number (Figure 8);
$F(X)$ the proportion of the total discharge that goes through throats where the variable Γ is smaller than X.

[43] The ranges of local velocities estimated by the model are in good agreement with the usual velocities observed during runoff on natural surface (~100 mm/s). Additionally, the slope and the inundation ratio do not seem to have a great influence on the ranges of estimated velocities.

[44] These statistical results point out two major characteristics of the flow, at least for the steepest slopes. On the one hand, the local Reynolds number at the throats that mainly contribute to the discharge is relatively low such that the flow can be interpreted as laminar (Figure 8) [*Savat*, 1980]. On the other hand, most of the contributing edges are critical such that the head loss is dominantly determined by hydraulic jumps and falls, i.e., by inertia (Figure 7). In other words, the resistance is not primarily due to viscous resistance or boundary friction. This is actually consistent with our understanding of overland flow hydraulics in that it is clear that Darcy-Weisbach equations based simply on Reynolds number effect and laminar resistance do not work [*Abrahams et al.*, 1986; *Lawrence*, 1997], even when the bulk Reynolds number for the entire flow field indicates that the flow regime is laminar. It is also consistent with field observations of partially inundated flows on rough surfaces, which frequently report the occurrence of disturbed free surfaces with localized hydraulic jumps [e.g., *Abrahams et al.*, 1986].

4.4. Global Discharge

[45] From the network and hydraulic models discussed in the previous section, we can estimate the discharge which would be associated with a particular inundation level at different slopes. For each slope considered, we find similar general trends in that the discharge increases until the inundation ratio reaches a value of one (Figure 9).

[46] However, for inundation values greater than one, the discharge decreases. This is not surprising, in that the network is based on a skeletal structure which becomes less relevant once the surface is fully submerged and distinct channels no longer dominate the flow. It is at this point that we would expect the model to break down, and the calculated discharges suggest that this is the case. This suggests that the domain of validity for the model is for partially inundated surfaces with inundation ratios lower than 0.8. It should also be noted that the pattern of discharge becomes much more variable with increasing slope. This is presumably due to the higher Froude numbers associated with a given depth on a higher slope, which in turn would

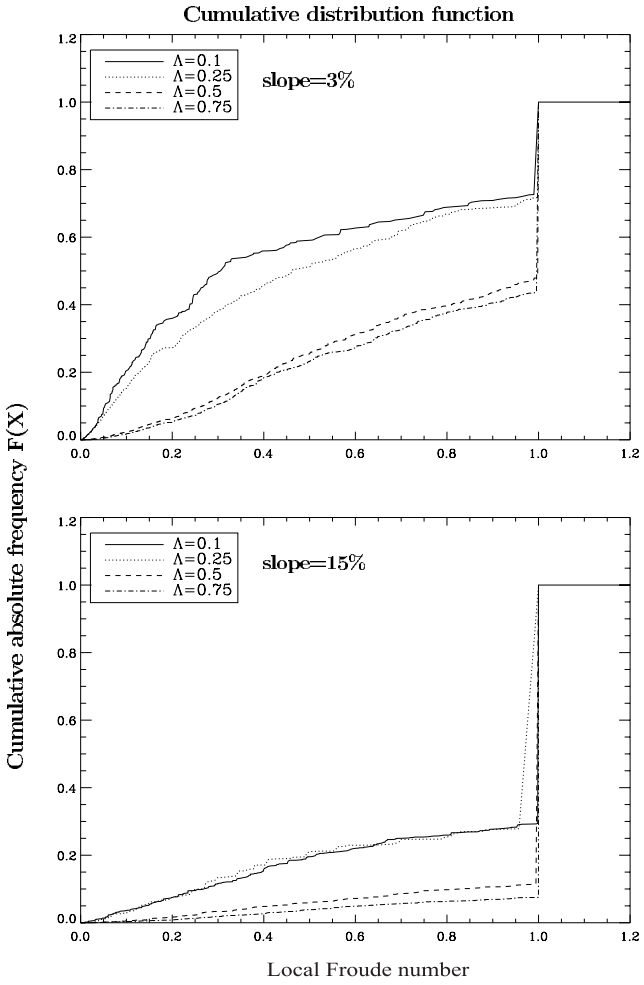

Figure 7. Froude number cumulative distribution function according to local discharges. $F(X)$ is the proportion of the total discharge that goes through throats where the Froude number Fr is smaller than X.

contribute to a higher frequency of localized critical flow (Figure 7).

[47] Note that on the one hand the model maximizes the frictional head losses in subcritical channels, since it is computed on the basis of the throat velocity instead of the mean velocity. On the other hand the model minimizes the frictional head losses in subcritical channels because they are regarded as smooth channels (for simplicity we have used Poiseuille and Blasius formulas in equation (7)) and we have ignored the transitional zone in the Moody diagram [*Moody*, 1944]. For testing the effect of this, a variable coefficient for all frictional head losses was introduced. The effect on the global discharge was found to be negligible, confirming that the global discharge is only weakly influenced by frictional head losses, in contrast with inertial losses in critical channels.

4.5. Darcy-Weisbach Coefficient

[48] Classically, the Darcy-Weisbach coefficient of the whole surface is defined by

$$f = \frac{2gD\sin(\theta)}{v^2} \tag{14}$$

where $\sin(\theta)$ is the surface slope. In applying this formula, a significant problem exists when defining the velocity v and of the hydraulic diameter of the whole surface D used in the case of partial inundation. In the previous sections of this paper, we have accounted for the complex microgeometry of the surface by using the HNM and the varying SRM. We have also shown that the magnitude of the local velocity is widely distributed. However, when modeling flow at the scale of a hillslope the microgeometry and associated velocity field cannot be easily accounted for at that scale. We therefore use an "average" global velocity of the form

$$v = \frac{q}{d} = \frac{Q}{wd} \tag{15}$$

where q is the specific discharge and Q the discharge over a sample of width w. Similarly, the hydraulic diameter is taken as $D = 4d$ as for a rectangular cross section of infinite width. This velocity can be interpreted as a flow density, similar to the Darcy velocity used in porous media flow and provides a simple quantity for comparative purposes.

[49] The Darcy-Weisbach coefficient obtained using these quantities is shown in Figure 10 as a function of the

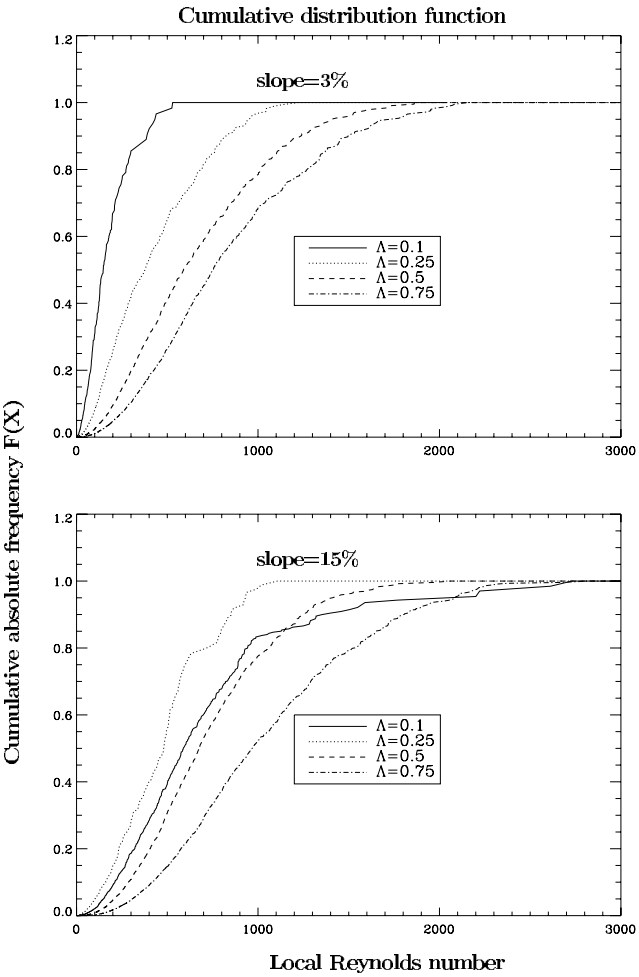

Figure 8. Reynolds number cumulative distribution functions according to local discharges. $F(X)$ is the proportion of the total discharge that goes through throats where the Reynolds number Re is smaller than X.

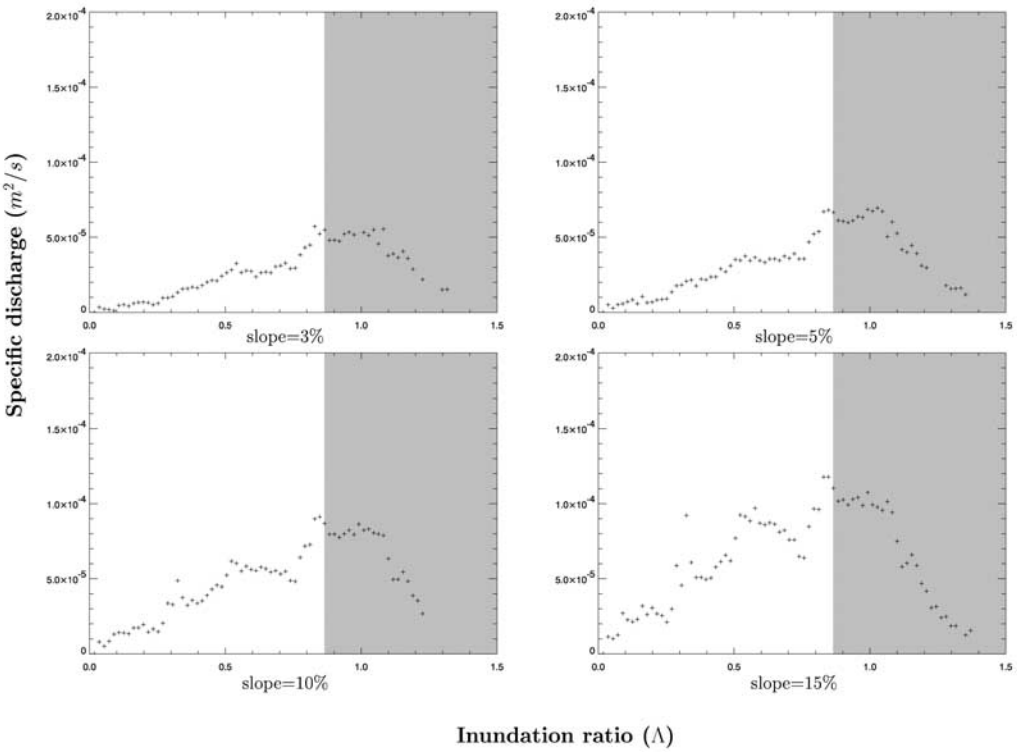

Figure 9. Discharges over the surface on inundation ratio basis. The model is no more valid in the shaded domain.

inundation ratio. Within the domain of validity of the numerical model (i.e., $\Lambda < 0.8$), the Darcy-Weisbach coefficient generally increases with the inundation ratio, although the trend is not entirely monotonic. The upward trend observed during partial inundation is similar to that observed in the compiled experimental results and in the drag resistance model proposed by *Lawrence* [1997, 2000]. In the modeling proposed here as well as in the drag model, the inertial head losses associated with local flow disturbances are dominant over friction and produce similar behaviors of the flow parameters. A nonnegligible dependence on the Reynolds number is also apparent in these results, with higher slopes producing lower values of resistance at a given flow depth (i.e., inundation ratio). This simply reflects the fact that for a fixed flow depth, the higher slopes will be associated with higher velocities, thus decreasing the apparent frictional resistance.

5. Conclusion

[50] Numerical simulation of overland flow under conditions of partial roughness inundation over a sample of a natural surface has been performed, on the basis of the knowledge of the roughness topology and the application of a hydraulic model for flow through the associated network. Such an approach accounts for the variation of the effective cross sections, flow pathways and the hydraulic roughness with inundation. The specific discharge has been computed as a function of the inundation ratio for various slopes and the Darcy-Weisbach coefficient for the global flow field has been derived. Consistent with published recent literature, it appears that the inundation ratio is the key parameter controlling the flow resistance, rather than Reynolds number, and that the Darcy-Weisbach coefficient increases with inundation ratio within the domain of partial inundation.

[51] Analysis of numerical data provides some indication of the possible local flow regime. Although local Reynolds number values do not clearly indicate that the flow is turbulent, as a great part of the global discharge goes through critical edges, head losses associated with local flow disturbances are dominated by inertia. Therefore a global Reynolds number calculated using the global dis-

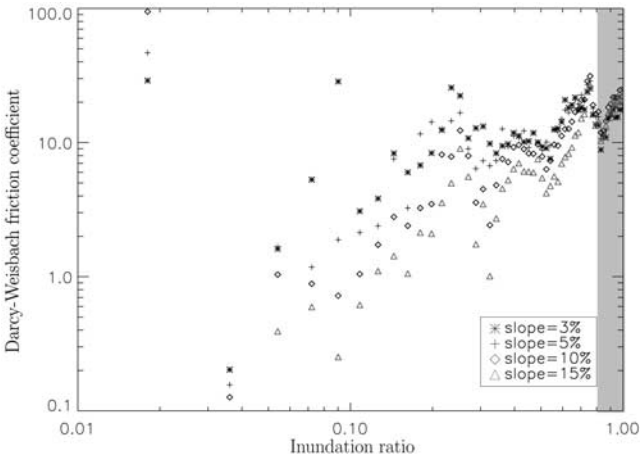

Figure 10. Darcy-Weisbach coefficient. There are outliers for the lowest inundation ratios because the Darcy-Weisbach coefficient is unspecified near the percolation threshold. Indeed, considering equation (14), as D and v tend toward zero, f is unspecified.

charge is definitely not a key parameter for characterizing the flow.

[52] In the present work we chose to account for the varying influence of roughness with inundation by the means of different networks. Within this context flow network structure has a large effect on global discharge. Further numerical work, using rough surfaces randomly generated with identical or different statistical properties than the surface considered in this paper, will enable us to better understand the influence of roughnesses spatial dispatching on the network, on the local flow configuration and eventually on the global discharge.

References

Abrahams, A. D., A. J. Parsons, and S.-H. Luk (1986), Resistance to overland flow on desert hillslopes, *J. Hydrol.*, *88*, 343–363.

Chassery, J. M., and A. Montanvert (1991), *Géométrie Discrète en Analyse d'Images*, Hermes, Paris.

Coster, M., and J. L. Chermant (1989), *Précis d'Analyse d'Images*, CNRS Press, Paris.

Dunne, T., and W. E. Dietrich (1980), Experimental study of Horton overland flow on tropical hillslope, 2. Hydraulic characteristics and hillslope hydrographs, *Z. Geomorphol.*, *35*, suppl., 60–80.

Einstein, H. A., and R. B. Banks (1950), Fluid resistance of composite roughness, *Eos Trans. AGU*, *31*, 603.

Emmett, W. W. (1970), The hydraulics of overland flow on hillslopes, *U.S. Geol. Surv. Prof. Pap.*, *662-A*, 68 pp.

Ferro, V. (2003), Flow resistance in gravel-bed channels with large scale roughness, *Earth Surf. Processes Landforms*, *28*, 339–1325.

Gilley, J. E., and S. C. Finkner (1991), Hydraulic roughness coefficients as affected by random roughness, *Trans. ASAE*, *34*(3), 897–903.

Gonzales, R. C., and R. E. Wood (1992), *Digital Image Processing*, Addison-Wesley, Boston, Mass.

Horton, R. E., H. R. Leach, and R. Van Vliet (1934), Laminar sheet-flow, *Eos Trans. AGU*, *2*, 393.

Kamphorst, E. C. (2000), Measurement and estimation methods of maximum depression storage on tilled soils, Ph.D. thesis, Inst. Nat. de la Rech. Agron., Paris.

Kurosh, A. G. (1972), *Higher Algebra*, translated from Russian by G. Yankovksy, MIR, Moscow.

Laurent, J. P., and C. Frendo-Rosso (1992), Application of image analysis to the estimation of AAC thermal conductivity, in *Advances in Autoclaved Aerated Concrete*, edited by F. H. Wittman, pp. 65–70, A. A. Balkema, Rotterdam, Netherlands.

Lawrence, D. S. L. (1997), Macroscale surface roughness and frictionnal resistance in overland flow, *Earth Surf. Processes Landforms*, *22*, 365–382.

Lawrence, D. S. L. (2000), Hydraulic resistance in overland flow during partial and marginal. surface inundation: Experimental observations and modeling, *Water Resour. Res.*, *36*, 2381–2393.

Lencastre, A. (1979), *Manuel d'Hydraulique Générale*, Eyrolles, Paris.

Leopold, L. B., and T. Maddock Jr. (1953), The hydraulic geometry of stream channels and some physiographic implications, *U.S. Geol. Surv. Prof. Pap.*, *525*.

Li, R.-M., and H. W. Shen (1973), Effect of tall vegetations on flow and sediment, *J. Hydraul. Div. Am. Soc. Civ. Eng.*, *99*(5), 793–814.

Moody, L. F. (1944), Friction factors for pipe flows, *ASME Trans.*, *66*, 671–684.

Phelps, H. O. (1975), Shallow laminar flows over rough granular surfaces, *Proc. Am. Soc. Civ. Eng.*, *3*, 367–384.

Pieritz, R. A. (1992), Modélisation et simulation de milieux poreux par réseaux topologiques, Ph.D. thesis, Univ. Joseph Fourier, Grenoble, France.

Rauws, G. (1980), Laboratory experiments on resistance to overland flow due to composite roughness, *J. Hydrol.*, *103*, 37–52.

Richards, K. S. (1973), Hydraulic geometry and channel roughness-a non linear system, *Am. J. Sci.*, *273*, 877–896.

Savat, J. (1980), Resistance to flow in rough supercritical sheet flow, *Earth Surf. Processes*, *5*, 103–122.

Takken, I., and G. Govers (2000), Hydraulics or interrill overland on rough bare soil surfaces, *Earth Surf. Processes Landforms*, *25*, 1387–1402.

U.S. Army Corps of Engineers (1994), Engineering and design–Flood-runoff analysis, *Eng, Manual 1110-2-1417*, Washington, D. C.

Woo, D. C., and E. F. Brater (1961), Laminar flow in rough rectangular channels, *J. Geophys. Res.*, *66*, 4207–4217.

Yoon, Y. N., and H. G. Wenzel (1971), Mechanics of sheet flow under simulated rainfall, *J. Hydraul. Div. Am. Soc. Civ. Eng.*, *97*(9), 1367–1386.

J.-F. Daïan and N. Roche, Laboratoire d'Étude des Transferts en Hydrologie et Environnement, Université Joseph Fourier, BP 53, F-38041 Grenoble Cedex 09, France. (nicolas.roche@hmg.inpg.fr)

D. S. L. Lawrence, School of Human and Environmental Sciences, University of Reading, Reading RG6 6AB, UK.